



Cite this: *Green Chem.*, 2023, **25**, 4769

## A lignin-based membrane fabricated with a deep eutectic solvent†

Abaynesh Yihdego Gebreyohannes,<sup>a,b</sup> Sandra L. Aristizábal,<sup>a,b</sup> Liliana Silva,<sup>a,c</sup> Eyad A. Qasem,<sup>d</sup> Stefan Chisca,<sup>a,b</sup> Lakshmeesha Upadhyaya,<sup>a,b</sup> Daniyah Althobaiti,<sup>a,b</sup> João A. P. Coutinho<sup>c</sup> and Suzana P. Nunes<sup>c</sup> \*<sup>a,b,d</sup>

Membrane technology is a sustainable process of molecular separation and purification in the chemical and pharmaceutical industries, with lower energy consumption than traditional thermal methods. For sustainability reasons, the membrane fabrication itself needs to align with the 12 principles of green chemistry with low environmental impact, preferentially using natural polymers and green solvents. Membranes are currently mostly produced from petroleum-based polymers and organic solvents like dimethylformamide, which are not expected to be used in large amounts anymore. Lignin is a natural green polymer option, however its low solubility in mild solvents has limited its processability into membranes. We propose a sustainable membrane fabrication method using lignin fully dissolved in a green deep eutectic solvent (DES). The crosslinking with 5% epoxide in the aqueous medium enhanced the membrane stability, enabling its application in an aqueous and organic solvent medium. The resulting membrane had a molecular weight cut-off of 1.3 kg mol<sup>-1</sup>, a range relevant to molecular separation in the pharmaceutical and chemical industries.

Received 24th February 2023,  
Accepted 28th April 2023

DOI: 10.1039/d3gc00658a

[rsc.li/greenchem](http://rsc.li/greenchem)

## Introduction

Membrane technology has become a sustainable separation process in the chemical and pharmaceutical industries with unique advantages of low energy consumption compared to thermal methods. The development of more stable membranes is allowing the extension of the application of the technology to processes in organic solvents, while their higher selectivity can shorten the steps of product purification. It has become a consensus that sustainability must be seen in a more holistic way. Besides the separation process, the membrane fabrication should be sustainable as well. As a matter of fact, membranes are currently mostly based on high-performance polymers obtained from fossil sources. The membrane fabrication is mainly a solvent-based process. Polymer dis-

solution requires a large volume of solvents like dimethylformamide, which are far from green. There has been increasing awareness and efforts to replace the traditionally used organic solvents with greener ones<sup>1</sup> and to substitute synthetic polymers with greener alternatives from biodegradable sources.<sup>2</sup> In this work, we are proposing a new system for membrane preparation constituted of a sustainable natural polymer, lignin, and a green deep eutectic solvent.

While high-performance polymers are regularly applied due to their processability and stability, their fabrication is linked to a high carbon footprint and when they are discarded, after fulfilling their function, their degradation may take several years.<sup>3</sup> Serious environmental damage is projected from an accumulation of over 11 billion metric tons of plastics in both aquatic and terrestrial environments by 2025.<sup>4</sup> Environmentally benign biodegradable biopolymers such as chitosan, starch, and those obtained from biomass including lignin, cellulose, or hemicellulose could significantly reduce the dependence on fossil fuels and the subsequent greenhouse gas emissions. Lignin is one of the most abundant natural polymers in the world. It is the only renewable aromatic raw material, although it is often regarded as a waste material in the processing of lignocellulosic biomass.<sup>5</sup> Particularly, the Kraft method in the pulp and paper industry generates a huge mass of lignin as a by-product, which is directly discharged or burnt as an energy source.<sup>6</sup> The amount of lignin by-products is anticipated to increase more with the implementation of

<sup>a</sup>Environmental Science and Engineering, Biological and Environmental Science and Engineering Division (BESE), King Abdullah University of Science and Technology (KAUST), 23955-6900 Thuwal, Saudi Arabia. E-mail: [suzana.nunes@kaust.edu.sa](mailto:suzana.nunes@kaust.edu.sa)

<sup>b</sup>Advanced Membranes and Porous Materials Center (AMPM), King Abdullah University of Science and Technology (KAUST), 23955-6900 Thuwal, Saudi Arabia

<sup>c</sup>CICECO – Aveiro Institute of Materials, Department of Chemistry, University of Aveiro, 3810-193 Aveiro, Portugal

<sup>d</sup>Chemical Engineering, Physical Science and Engineering Division (PSE), King Abdullah University of Science and Technology (KAUST), 23955-6900 Thuwal, Saudi Arabia

† Electronic supplementary information (ESI) available. See DOI: <https://doi.org/10.1039/d3gc00658a>



second-generation biofuels and chemicals from biomass.<sup>7</sup> Lignin, due to its cheap natural abundance, nontoxicity, biodegradability, and renewability, is an interesting material for producing eco-friendly membranes, as we transition from linear to circular economy.<sup>8</sup> However, its market share as a polymeric product has been negligible due to its complexity and difficult processability in solution. Lignin has been previously considered for membranes, but its success has been limited. According to Xia *et al.*,<sup>9</sup> the two most common strategies to incorporate lignin into membrane manufacture are (i) lignin as such, which may lead to poor performance, (ii) defragmentation to monomers, which are then polymerized, which is costly and increases the steps of the process. The dissolution of lignin to form a homogeneous solution and subsequently a polymeric membrane film has involved the use of harmful chemicals and a complex process that incur high operational costs.<sup>2</sup> For the lignin membranes reported so far, an additional limitation has been its poor mechanical stability, which was in part overcome by blending it with other polymers (lignin/polyvinyl alcohol)<sup>10</sup> during the manufacturing process, interfacial polymerization of alkali lignin as a water-soluble monomer exposed to acyl chloride in the organic phase,<sup>11</sup> and layer by layer assembly of sulfonated lignin sodium salt with poly(diallyl dimethyl ammonium chloride).<sup>12</sup> Therefore, it is highly imperative to develop a simple environmentally friendly method to dissolve lignin and manufacture it into robust membranes for a broad range of separation and purification applications.

Herein, we report for the first time the dissolution of the naturally abundant lignin in an environmentally friendly deep eutectic solvent (DES) and the manufacture of membranes therefrom. DESs have become an exciting alternative to the more expensive ionic liquids (ILs). They are constituted of a homogeneous mixture of two solid-phase chemicals that form a joint superlattice at a particular molar ratio with a melting point signifi-

cantly lower than that of the individual components. When measuring the melting temperature as a function of the mixture molar fraction, a deep crevice is observed at the eutectic point. DESs are mainly composed of a quaternary ammonium salt and a complexing agent, interacting through hydrogen bonds.<sup>13</sup> They are considered green solvents due to their low volatility, low toxicity, biodegradability, and biocompatibility. They can be easily prepared with tunable properties at high purities due to 100% reaction mass efficiency, non-flammability, and widely available precursors (amides, carboxylic acids, and alcohols) or metal chlorides (ZnCl<sub>2</sub>, SnCl<sub>2</sub>, FeCl<sub>3</sub>, *etc.*).<sup>13,14</sup> Biocompatible ingredients which can be sustainably extracted from biomass to form DESs are formic acid, lactic acid, and acetic acid.

Driven by their interesting properties, DESs started to be explored for membrane fabrication. Excellent reviews of recent approaches have been published by Castro-Muñoz *et al.*<sup>15</sup> and Taghizadeh *et al.*<sup>16</sup> Table 1 summarizes the selected examples of DESs applied in the membrane preparation and modification and the main achievements. So far, DESs have been mainly used integrated into supported liquid membranes and as an additive or as a co-solvent for membrane casting in combination with other solvents. This work is the first report of (i) a DES used as a single solvent for polymer solution casting in a membrane fabrication process, (ii) dissolution of lignin in the DES to form a homogeneous solution of polymer concentration up to 25 wt%, and (iii) preparation of pure lignin-based membranes by dissolution and casting by a fully green process.

## Materials and methods

### Materials

Kraft lignin (alkali) was purchased from Sigma Aldrich. Poly(ethylene glycol) (PEG) (0.4, 1.5, 10, and 35 kg mol<sup>-1</sup>),

**Table 1** Examples of DESs used in membrane fabrication

Purpose	DES type	Main achievement	Ref.
Pore-forming additive (0–4%) for the polyethersulfone membrane	Imidazole-based decanoic acid/tetrabutylammonium chloride	Narrow pore-size distribution, smooth surface	17 and 18
Post-treatment of polyamide membrane interfacial polymerization selective layers	Choline chloride, ethylene glycol, urea, and glycerol	Smooth and wettable surface with higher permeance	19
Additive (0–4%) for polyethersulfone/polyvinylpyrrolidone membrane casting	Ethylene glycol, choline chloride	Narrow pore-size distribution, enhanced performance	20
Polyimide ultrafiltration membranes filled with DES-embedded silica (<2.5%)	Choline chloride, ethylene glycol	Enhanced phenol separation	21
Silk nanofiber exfoliation for supercapacitor separators	Urea/guanidine hydrochloride	Enable preparation of silk-based membranes	22
Additive (1–10%) to <i>m</i> -phenylene diamine in the aqueous phase of the preparation of polyamide membrane selective layers by interfacial polymerization	Choline chloride, urea	Smooth and hydrophilic surface	23
Graphene oxide functionalization	Choline chloride, ethylene glycol	Improved water permeance with high salt rejection	24
Co-solvent for poly(vinylidene fluoride) and polyacrylonitrile membrane preparation	Benzyl-trimethylammonium mesylate/ <i>p</i> -toluene sulphonic acid mono hydrate; phenyl acetic acid/trimethyl glycine; glycolic acid/trimethyl glycine	Co-solvent for membrane casting in combination with other green solvents	25



$\gamma$ -cyclodextrin ( $1297 \text{ g mol}^{-1}$ ), propionic acid, urea, acetone, 1,4-butanediol diglycidyl ether (BDDE), and all other organic solvents were obtained from Arcos. Trimethylolpropane ethoxylate  $1 \text{ kg mol}^{-1}$  was acquired from Sigma Aldrich.

### Lignin dissolution

A deep eutectic solvent (DES) was prepared by mixing propionic acid and urea in a 2 : 1 ratio and stirring at ambient temperature until a clear solution was obtained (Fig. S1†). This solvent was selected based on its demonstrated technical lignin dissolution capacity.<sup>26,27</sup> The solution remained liquid at room temperature. Depending on the percentage of water molecules, the DES can be solvated and negatively affects the dissolution of lignin. Hence, 25 wt% alkali lignin was first dried in an oven at  $80^\circ\text{C}$  and then mixed with the freshly prepared DES. The mixture of the solvent and lignin was flushed with dry  $\text{N}_2$  to void water absorption into the solution compromising the solubility and stirred at  $90^\circ\text{C}$  until a homogeneous solution was obtained.

### Membrane preparation

The membranes were prepared by nonsolvent-induced phase separation (NIPS). Solutions of 22 wt% lignin in DES were cast on a glass plate using a doctor blade with a  $200 \mu\text{m}$  gap and water as the coagulation bath. The concentration was chosen to combine stability aligned to low transport resistance. To minimize swelling in an aqueous medium and increase the membrane stability, a green crosslinking strategy was employed, by using 5% BDDE in water at  $80^\circ\text{C}$  for 24 h, as previously applied to polytriazole with hydroxyl groups.<sup>28</sup> The procedure is presented in Fig. 1.

### Characterization methods

**Spectroscopic characterization (NMR, UV-VIS).** Nuclear Magnetic Resonance (NMR) spectra were obtained on a Bruker

Avance-III 500 MHz spectrometer with a Z-axis gradient BBO probe using  $\text{DMSO-d}_6$  as the solvent for  $^1\text{H}$  and  $^{13}\text{C}$  experiments. The crosslinking reaction was confirmed by  $^{13}\text{C}$  cross-polarization-magic angle spinning (CP-MAS) solid-state NMR, recorded on a Bruker AVANCE III spectrometer operating at 400 MHz.

**Thermal and mechanical analyses (TGA, DSC, DMA).** Thermogravimetric analysis (TGA) was used to evaluate the thermal stability of the membrane from  $35^\circ\text{C}$  to  $1000^\circ\text{C}$  with a heat ramp of  $20^\circ\text{C min}^{-1}$  under an air and nitrogen atmosphere, using a TA Instruments Q5000 analyzer. Differential scanning calorimetry (DSC) was performed on a TA DSC-Q20, from  $35$  to  $250^\circ\text{C}$  with a rate of  $10^\circ\text{C min}^{-1}$  under an inert atmosphere, to remove the thermal history of the polymer and then an increase from  $40$  to  $220^\circ\text{C}$  with a rate of  $20^\circ\text{C min}^{-1}$  to measure the glass transition temperature,  $T_g$ .

Tensile strength and elongation were measured on a dynamic mechanical analysis (DMA) TA instrument DMA 850, equipped with a humidifier, at a tensile rate of  $0.1 \text{ N min}^{-1}$ . Starting from a dry membrane, we stepwise increased the relative humidity up to 80%, close to saturation. The results are an average of four different membrane samples prepared under the same conditions.

**Membrane surface and morphological characterization.** The water contact angle was measured on a drop shaper analyzer (KRÜSS, DSA100E) equipped with a monochrome interline CCD camera. An injection of  $2 \mu\text{L}$  of water was done on the sample surface for each measurement. The contact angle was automatically calculated by the Elipse (Tangent-1) method.

The morphology of the membranes was characterized by scanning electron microscopy (SEM) (on a Quattro FEI microscope). Atomic force microscopy (AFM) was used to image the surface and determine the roughness in tapping mode (AFM, Bruker Dimension Icon SPM) with a ScanAsyst – air probe, after fixing the sample on a glass slide.

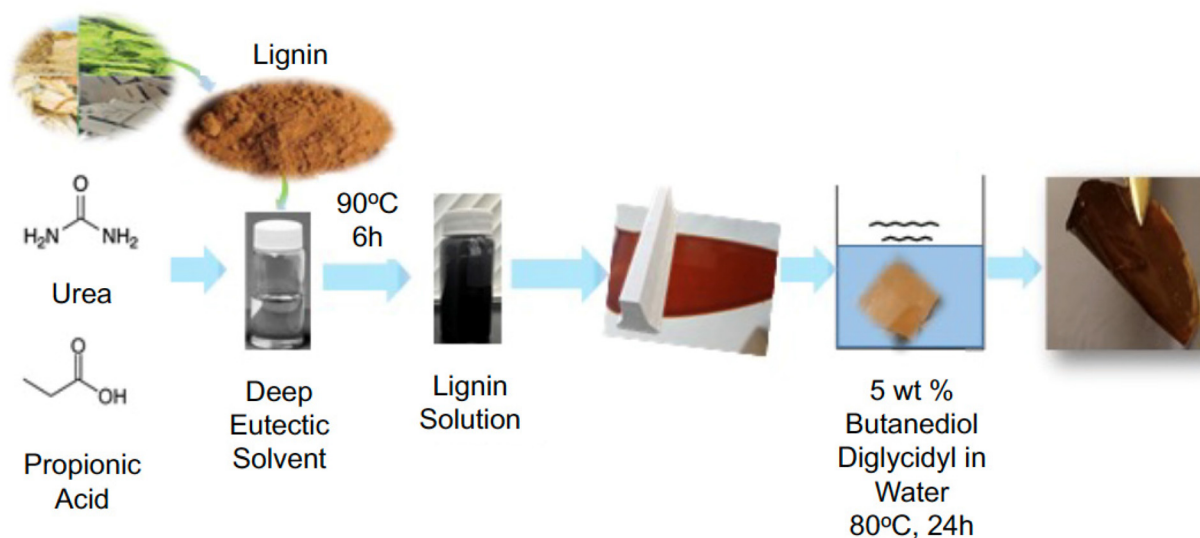


Fig. 1 Schematic representation of the membrane preparation and crosslinking procedure.



**Membrane performance.** The flat-sheet membrane was fitted into a dead-end filtration cell to measure its performance at 18.8 bar and ambient temperature. A 1 g L<sup>-1</sup> mixture of different molecular weight linear PEGs (0.4, 1, 1.5, 10 and 35 kg mol<sup>-1</sup>), or individual solutions of branched PEG (1 kg mol<sup>-1</sup>),  $\gamma$ -cyclodextrin (1.297 kg mol<sup>-1</sup>), trimethylolpropane ethoxylate (1 kg mol<sup>-1</sup>) or Rose Bengal (1.018 kg mol<sup>-1</sup>) in water were used as model solutes to determine the molecular weight cut-off (MWCO) of the membrane. Aliquots of feed, permeate and retentate samples were analyzed by gel permeation chromatography (Agilent GPC-Aqua RID). The GPC is equipped with an Agilent refractive index detector and uses water as the mobile phase at 35 °C. Feed, permeate, and retentate dye solutions were analyzed on a UV-VIS spectrometer (NanoDrop 2000c, Thermo Scientific).

The rejection was calculated using eqn (1), where  $C_f$  and  $C_p$  correspond to the concentration in the feed and permeate.

$$R = \left(1 - \frac{C_p}{C_f}\right) \times 100\% \quad (1)$$

## Results and discussion

Membranes fully based on lignin, which is a biopolymer with phenol and hydroxyl functional groups,<sup>29</sup> were fabricated by NIPS. The used solvent for lignin was a green DES constituted of propionic acid and urea, which are a hydrogen bond donor-acceptor. The two DES components were mixed at room temperature and form a stable transparent solution (Fig. S1†). Both the acidic nature and rich hydrogen bonding of the DES promoted a fast dissolution of up to 25 wt% Kraft lignin at 80 °C. The homogeneous viscous solution is shown in Fig. S1.† The dissolution takes place by the protonation of the C $\alpha$ -OH group of lignin under acidic DES, followed by dehydration to form a C $\alpha$  cation intermediate.<sup>30</sup>

Changing the pH or the ionic strength of the medium can induce the formation of large lignin aggregates. To form a homogeneous three-dimensional network, crosslinking is crucial.<sup>6</sup>

The crosslinking reaction applied in this work was performed in water using BDDE. Therefore, also the crosslinking process can be considered green as far as the conditions are concerned. It occurs by an epoxy ring opening in the presence of the phenol groups of the lignin to form an ether network. The chemical structure of a fragment of the lignin polymer is presented in Fig. 2. The successful incorporation of the crosslinking BDDE segment was confirmed by NMR. The crosslinkers' structure and the NMR characterization are presented in Fig. 2b.

In the solid-state <sup>13</sup>C NMR comparison (Fig. 2b), after the crosslinking reaction, the disappearance of the signals at around  $\delta$  = 50.7 and 43.8, and the intensity increase of the signals at around  $\delta$  = 73.1 and 27.3 ppm from the aliphatic carbons of the BDDE confirms the epoxy ring opening of the crosslinker. A decrease in the signal at around  $\delta$  = 147.9 ppm

from the phenolic carbon C-O with a slight shift to  $\delta$  = 148.2 ppm is also observed, analogously to similar reactions reported in the literature.<sup>24</sup> Other signals are from the carbonyl group at  $\delta$  = 172 ppm, the aromatic carbon region from  $\delta$  = 148–103 ppm, the aliphatic region below  $\delta$  = 95 ppm, a broad signal from the carbons next to ether bonds or oxygen from  $\delta$  = 79 to 67 ppm, and the characteristic signal of the carbon in the methoxy group at 56 ppm. Below  $\delta$  = 38 ppm are the signals from the saturated aliphatic carbons CH and CH<sub>2</sub>. The carbonyl presence can be related to the possible esterification of some aliphatic OH by remaining free propionic acid molecules at high temperature during the polymer dissolution and crosslinking.<sup>31</sup> Lignin has a complex polyphenolic heterogeneous chemical structure made from arylglycerol ether bonds between phenolic *p*-coumaryl, coniferyl, and sinapyl alcohol. It is known that the  $\beta$ -aryl ether linkage ( $\beta$ -O-4') is the most abundant linkage (Fig. 2). Some of the functional groups are present both in the lignin and BDDE (ether, alcohol, and aliphatic carbons) and are overlapped (Fig. 2b). The proposed signal assignments are depicted in Fig. 1, and further studies of the reactivity and ratio of the aliphatic OH and phenolic OH groups can be found in the literature.<sup>32–34</sup>

Other evidence of a successful crosslinking is the solvent, thermal, and mechanical stability. After crosslinking, the membranes are stable in common organic solvents such as acetone, acetonitrile, alcohols (methanol, ethanol, isopropanol), toluene, hexane, dimethylformamide (DMF), and tetrahydrofuran (THF) under static conditions. The membrane remained stable in all solvents even after 8 weeks (Fig. S2†).

To evaluate the stability of the crosslinked membrane in different solvents, the swelling and gel contents were measured for crosslinked membranes prepared from 22 wt% lignin solutions and soaked in water, methanol, and acetone. The degree of swelling (eqn (S1)†) for water, methanol, and acetone was 99%, 200%, and 50% with a solvent uptake of 1, 2.5, and 0.64 cm<sup>3</sup> g<sup>-1</sup> respectively. This is not surprising, considering the higher polar affinity of methanol to the membrane (Table S1†). For the fully crosslinked membrane, the polymer-polymer intermolecular forces inhibit further dissolution with close to negligible weight loss after drying the swollen membrane at 60 °C under vacuum for 24 h.

Fig. 3a shows the TGA analysis of the membranes with and without crosslinking. The first weight loss for the cross-linked membrane started at 295 °C with a sharp decrease, whereas the pristine lignin membrane has a slow weight decrease starting at a temperature lower than 200 °C. The 2% weight loss at temperatures lower than 100 °C is due to dehydration, and the subsequent weight loss until 180 °C could be related to impurities from carbohydrates or sulfur-based species<sup>35</sup> (Fig. 3a and Table 2). The thermal treatment of lignin in the temperature range of 150–270 °C is accompanied by a condensation process with the participation of the OH groups of lignin. These processes might lead to the formation of unsaturated C=C and C-C bonds, which enhances the yield of the residual char at high temperature. Therefore, since the crosslinking strategy creates ether bonds with the consumption of the OH



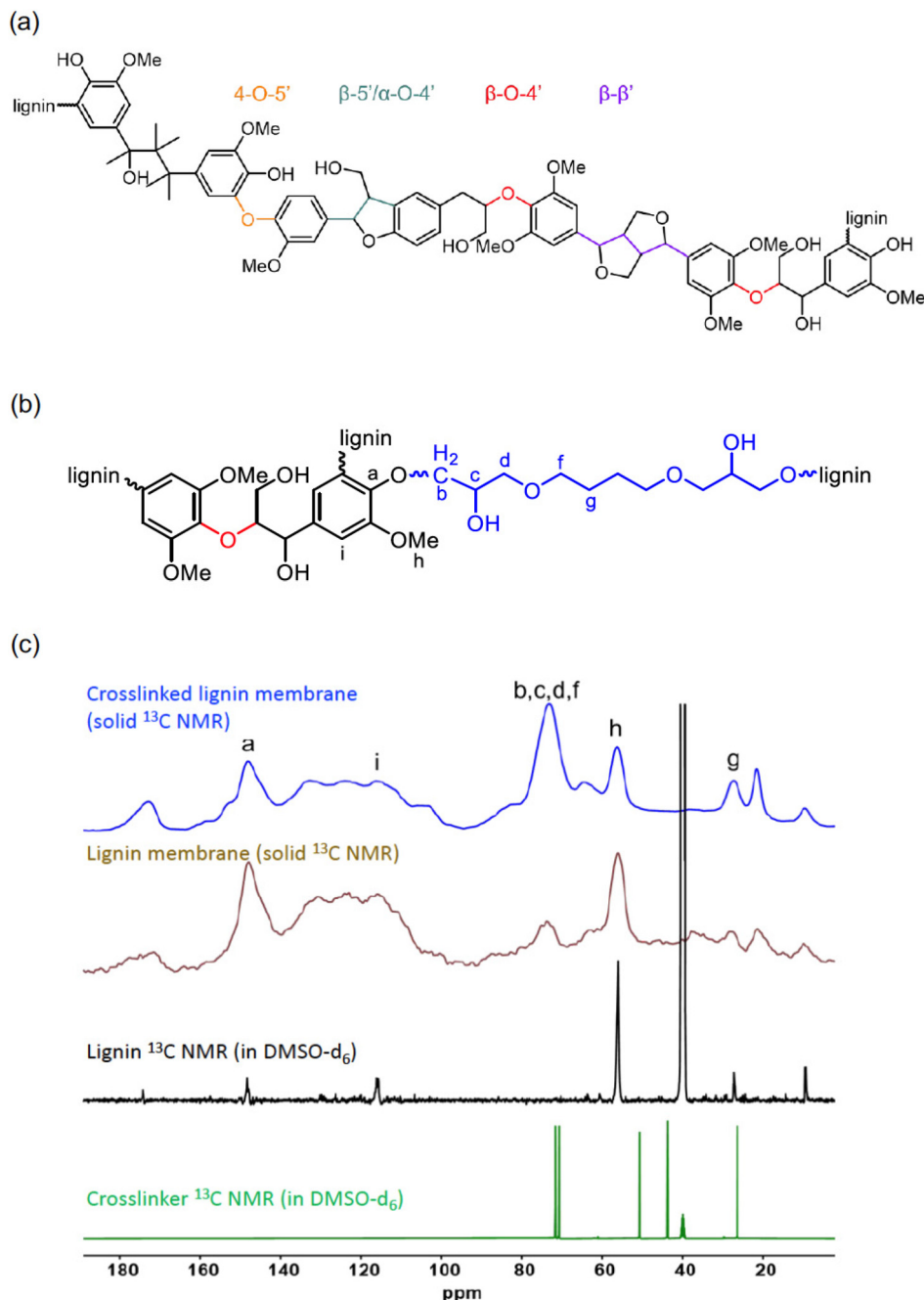


**Fig. 2** Chemical structures of (a) pristine and (b) cross-linked lignin, and (c) the corresponding NMR characterization: solid-state <sup>13</sup>C NMR spectra of the pristine lignin membrane (brown) and the membrane after crosslinking (blue); liquid <sup>13</sup>C NMR spectra of lignin (black) and the crosslinker (green) in DMSO-d<sub>6</sub>.

groups, the char yield is lower in the crosslinked membrane. The DSC analysis (Fig. 3b–d) shows in the first heating run an endothermic peak due to dehydration below 110 °C. The second heating run shows a  $T_g$  of 92.7 °C for the pristine lignin and 93.4 °C for the cross-linked membrane. Since  $T_g$  depends on the mobility of the polymeric chains (free volume, cohesive energy, and crosslink density), it is reasonable that the membrane would have a slightly higher  $T_g$  after crosslinking.

Dry pristine and cross-linked membranes are brittle due to the highly aromatic structure of the amorphous film. When exposed to humidity, the membrane flexibility clearly increases, enabling an easy handling and full mechanical characterization. Stress–strain curves, tensile strengths, tensile strain, Young's modulus, and toughness were measured for the crosslinked membrane. The humidity was increased starting from 0% up to 80% relative humidity, close to the saturation. Above 40% relative humidity, the membranes were flex-





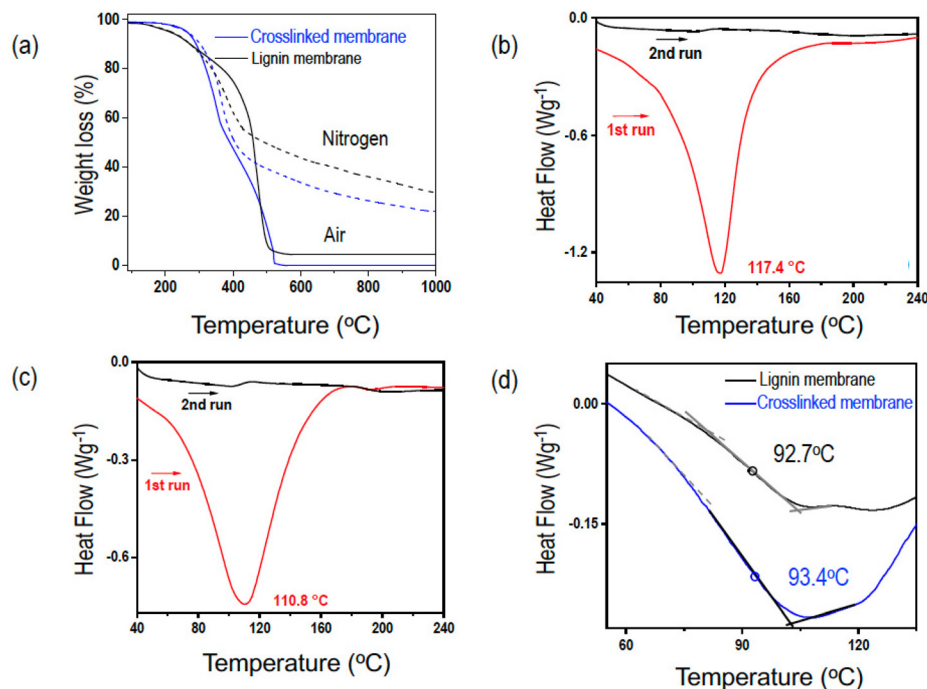


**Fig. 3** Thermal analysis. (a) TGA of pristine and cross-linked membranes under air and nitrogen. (b–d) DSC of lignin membranes ( $10\text{ }^{\circ}\text{C min}^{-1}$  temperature increase) (a) without and (c) with crosslinking; (d)  $T_g$  measurement for the pristine and crosslinked membranes ( $20\text{ }^{\circ}\text{C min}^{-1}$  temperature increase, second run).

**Table 2** TGA of lignin membranes before and after crosslinking

	$T_{10\%}$ ( $^{\circ}\text{C}$ )		Char yield <sub>1000 °C</sub> (%)	
	Air	N <sub>2</sub>	N <sub>2</sub>	Air
Pristine membrane	273	273	30	4
Crosslinked membrane	291	303	22	0

ible enough for reproducible DMA measurements, as shown in Table 3. The membranes have a complete elastic deformation (linear correlation between stress and strain) before breaking. As the relative humidity increases from 40 to 80%, the membrane toughness increases from 18 to 31  $\text{kJ m}^{-3}$ .

Lignin has an amphiphilic character due to its polar hydrophilic phenolic hydroxyl side groups and non-polar hydrophobic backbone.<sup>9</sup> Particularly, alkali lignin has a relatively

high oxygen content, which makes it convenient for chemical modification. The polar hydrophilic groups reacted leading to crosslinking, when exposed to a 5% BDDE solution in water at  $80\text{ }^{\circ}\text{C}$  for 24 h to provide mechanical strength. Since the crosslinking is performed in water, the method is more sustainable than other possible options like using diamines or dihalogenate derivatives, in acetonitrile or *n*-heptane. The water contact angle on a pristine lignin membrane surface is  $66^{\circ}$ . It increases to  $76^{\circ}$  after crosslinking due to the partial consumption of the OH groups and the addition of an aliphatic carbon chain (Fig. S3†).

### Membrane morphology

Kraft lignin is a result of a rigorous pulping process, which may result in low molecular weight polymer chains.<sup>6,32</sup> The low molecular weight leads to a low entanglement between chains and easy film disruption. Crosslinking in part compensates this effect and enhances the mechanical stability. Besides that, the incorporation of the aliphatic segments of crosslinkers might contribute to increase the flexibility of the lignin membranes, which have a high content of aromatic groups.

The SEM images of the membrane cross-section and surface before crosslinking (Fig. 4a and b) show an asymmetric porous morphology frequently observed by casting and immersion in a coagulation bath (NIPS).<sup>36</sup> The applied DES has a low viscosity and high affinity for water. This contributes to a fast solvent–non solvent exchange during the membrane fabrica-

**Table 3** Mechanical characterization of the crosslinked membranes cast from a 22 wt% lignin solution in DES

Relative humidity (%)	Tensile strength (MPa)	Tensile strain (%)	Young modulus (MPa)	Toughness ( $\text{kJ m}^{-3}$ )
40	$2.1 \pm 0.1$	$1.4 \pm 0.3$	$152 \pm 21$	$18 \pm 6$
80	$2.3 \pm 0.4$	$3.1 \pm 0.8$	$163 \pm 36$	$31 \pm 13$



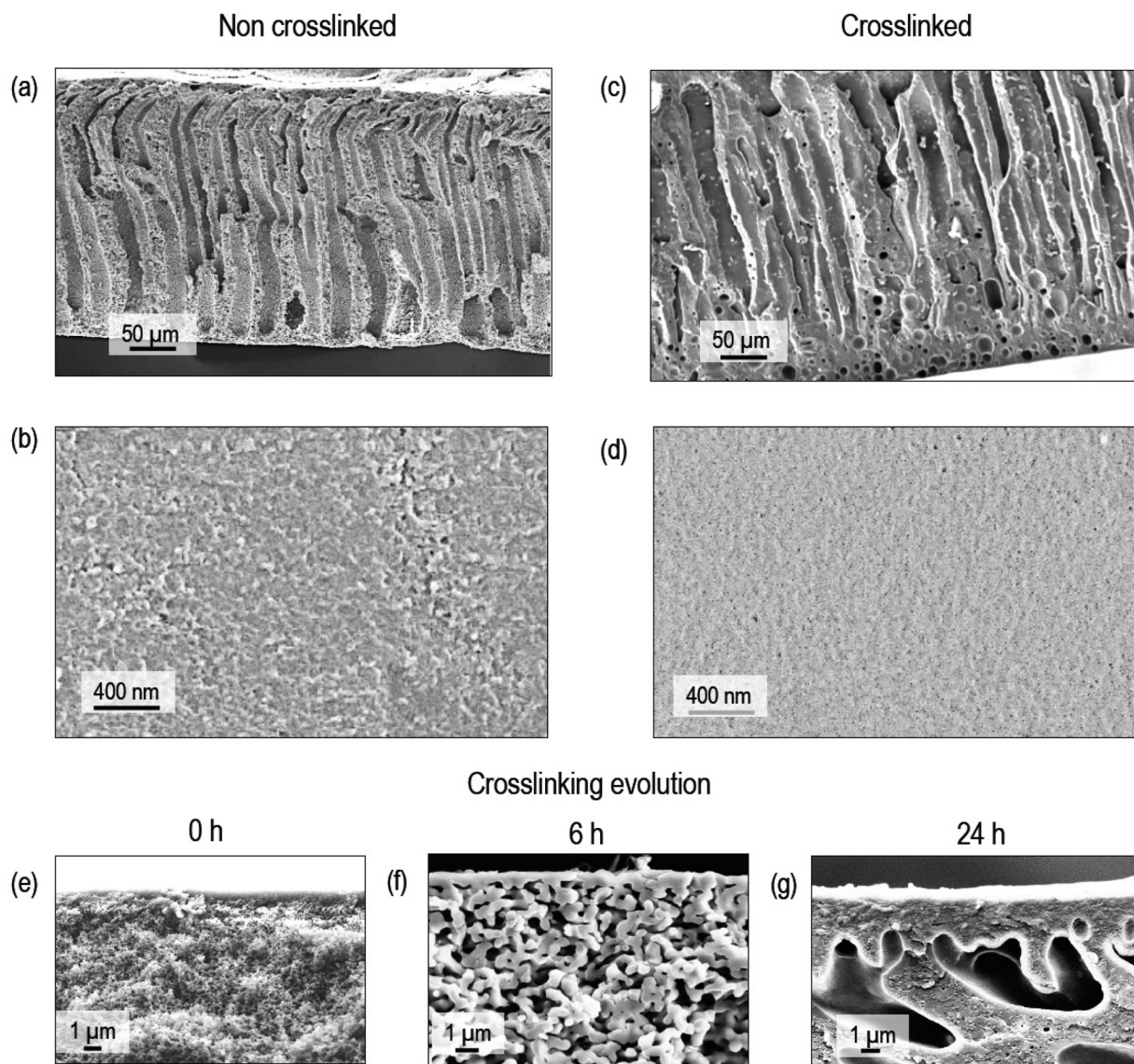


**Fig. 4** Cross-section and surface SEM images of membranes cast from 22 wt% lignin solution in DES (a and b) before (c and d) after crosslinking with 5% BDDE in water. (e–g) Cross-section SEM images of membranes with different crosslinking times: (e) 0, (f) 6, and (g) 24 hours. Crosslinking reaction with 5% 1,4-butanediol diglycidyl ether.

tion to create a highly porous finger-like structure. After crosslinking, there is clear densification in the overall structure, with a more pronounced effect on the surface (Fig. 4c and d). The membrane surface observed under a higher magnification AFM (Fig. S4†) has a well-defined granular morphology, which becomes more diffuse after crosslinking. This might be linked to the densification observed on the surface by SEM. The high-magnification SEM cross-sectional images (Fig. 4e–g) of membranes with different crosslinking times show how the morphology evolves with the time of immersion in the crosslinker solution. Voids are visible close to the membrane surface side, which has a very dense distribution of small pores. When immersed in the aqueous crosslinking solution, the membrane swells and at the same time the crosslinker penetrates it

promoting the crosslinking reaction. A crosslinker concentration gradient forms from the membrane surface to the bulk. In water, the polymer chains have high flexibility. As the crosslinking proceeds, interchain bridges are formed with a local densification in the swollen lignin layer close to the surface. As the chains approximate to be bridged, they leave a polymer depleted volume in other parts of the layer. Far from this region, the pores are larger from the beginning and interchain bridging can only occur in the thin pore walls, which might densify and lead to a minor increase of the pores, whose size is already larger, and the effect is less evident. These voids seem not to compromise the membrane selectivity, as seen in the performance characterization discussed below. Membranes prepared with 20 wt% lignin are more porous



than those prepared from 22 wt% solutions (Fig. S5†). The thickness of the membrane prepared from a 20 wt% lignin solution after crosslinking reduced to  $130 \pm 2 \mu\text{m}$  from an original value of  $150 \pm 1 \mu\text{m}$ . After a sequential filtration of water, methanol and acetone through the crosslinked membrane (22 wt% lignin), the cross-sectional SEM images show some compaction due to the high transmembrane pressure with a smoother surface (Fig. S6†).

### Membrane performance

In a circular economy, we aim at enabling any by-product to be recycled or transformed for another application. This work is an example of valorization of lignin into a high-added-value material, which could be useful in shape, size, or affinity-based molecular fractionation and solvent recovery as major targets in resource recovery in the pharmaceutical industry,<sup>37</sup> biorefineries,<sup>38–40</sup> and solid waste management. For instance, renewable biomass raw materials and related biomolecules are different in terms of chemical reactivity and separation process applicability from fossil-based sources. They have limited resistance to the high temperature required in distillation or gasification while also being less volatile due to their high molecular mass. Hence, membrane technology is beneficial for the upstream pretreatment processes of the renewable-based production system and low-temperature fractionation of chemically or biotechnologically transformed molecules.<sup>8</sup> Significant progress is needed in the development of biodegradable membrane materials compatible with harsh, aggressive solvents, with possible affinity to the mixture.

The lignin membrane had high chemical stability in a broad range of organic solvents under static conditions (Fig. S2†). For the filtration performance, the permeance of organic solvents and the size and shape selectivity of model solutes were tested. Before the filtration of pure organic solvents or aqueous solutions, the membrane was subjected to permeation of water at 19 bar until a constant flux. The cross-linked membrane had a water permeance of  $0.5 \pm 0.1 \text{ L m}^{-2} \text{ h}^{-1} \text{ bar}^{-1}$ .

Fig. 5a shows the permeance of a membrane cast from a 22 wt% lignin solution to water, methanol, and acetone. Fig. 5b shows a long-term permeance test for methanol conducted with a membrane cast from 20 wt% lignin. The methanol permeance over a long-term continuous operation at 19 bar was in this case constant at  $14 \text{ L m}^{-2} \text{ h}^{-1} \text{ bar}^{-1}$ .

Fig. 5a shows that the permeances of water and organic solvents through this membrane are not linearly proportional to the inverse of the solvent viscosity, indicating that they are not the result of pure viscous flow. The molecular weight of the solvents increases in the order of water < methanol < acetone and a simple correlation with the permeance is not linear either. These results indicate that the transport might strongly depend on other factors like the interaction between permeants and lignin. The polarity of the solvents decreases in the order of water > methanol > acetone. To better understand a possible contribution of the permeant–polymer interactions to the transport, we plotted the permeance as a function of the

product of the inverse of the viscosity multiplied by the inverse of the solvent molar diameter and by the polar (or hydrogen bond) contribution of the Hansen solubility parameter ( $\delta_{\text{p}}$  and  $\delta_{\text{H}}$ , respectively) (Fig. 5c and d).<sup>41</sup> The  $\delta_{\text{p}}$  and  $\delta_{\text{H}}$  values are listed in Table S1.† A more linear correlation is observed than when plotted simply as a function of the inverse of viscosity (Fig. 5a). This is an indication that particularly hydrogen bonding interactions have a predominant effect on transport, which is understandable, considering the large number of hydroxyl groups in lignin. Size and shape are relevant as well, considering the differences in rejection (Fig. 5e and Table 4). The bulky cyclodextrin molecule is more effectively rejected than linear molecules of similar size. Branched PEG is better rejected than linear analogs. Comparing solutes of similar size like  $1000 \text{ g mol}^{-1}$  poly(ethylene glycol) (PEG), the hyper-branched molecule has better retention (68%) than the linear molecule (30%). Similarly, the membrane rejects only  $33 \pm 7\%$  of linear PEG  $1.5 \text{ kg mol}^{-1}$  but rejects  $90 \pm 2\%$  of  $\gamma$ -cyclodextrin (molecular weight  $1.3 \text{ kg mol}^{-1}$ ) (Fig. 5e). The adsorption of dye molecules like Rose Bengal was in all cases less than 10%.

The performance of the membrane proposed here is compared with others reported in the literature in Table 5 for solvent permeance and rejection of molecules larger than  $800 \text{ g mol}^{-1}$  (Table 5). The permeance of the crosslinked lignin membrane (prepared from a 22 wt% lignin solution) to methanol ( $0.14 \text{ L m}^{-2} \text{ h}^{-1} \text{ bar}^{-1}$ ) is in the range of several other integral asymmetric membranes, but lower than that of thin-film composite membranes. The main achievement of our work is the demonstration that a DES can be used as a solvent for membrane fabrication without addition of a co-solvent.

Here we discuss the perspective applicability of this membrane in lignin fractionation and solvent recovery in biorefinery. Lignin valorization through the deconstruction of lignocellulosic biomass using organic solvents is a major strategy. The defragmented “lignin oil” is composed of monophenols (vanillin, methyl vanillate, *etc.*) and oligomers (*e.g.* 2-benzylphenol, benzyl phenyl ether) of low molecular weight mixed with molecules larger than  $1 \text{ kg mol}^{-1}$ . These components are the largest naturally occurring aromatic compounds, often regarded as by-products, but can be valorized as alternatives to fossil-based aromatic materials like bisphenols.<sup>57</sup> Several membranes have been employed to fractionate lignin by molecular weight range.<sup>38,39,58</sup> The defragmented mixture, especially from organo-solvent processes, also contains solvents. Distillation for solvent recovery is not economically competitive due to its high energy consumption. In a biorefinery, for lignin defragmentation, the desired membrane should have good selectivity between high ( $>1 \text{ kg mol}^{-1}$ ) and low ( $<1 \text{ kg mol}^{-1}$ ) molecular weights, stability towards organic solvents such as ethanol and methanol at high pressure, higher permeance, and low susceptibility to fouling.

The membrane separation of complex biomass-derived mixtures is highly dependent on the trilateral interaction between the membrane material, solvent, and solute. The literature reports that fully aromatic membranes are more effective in





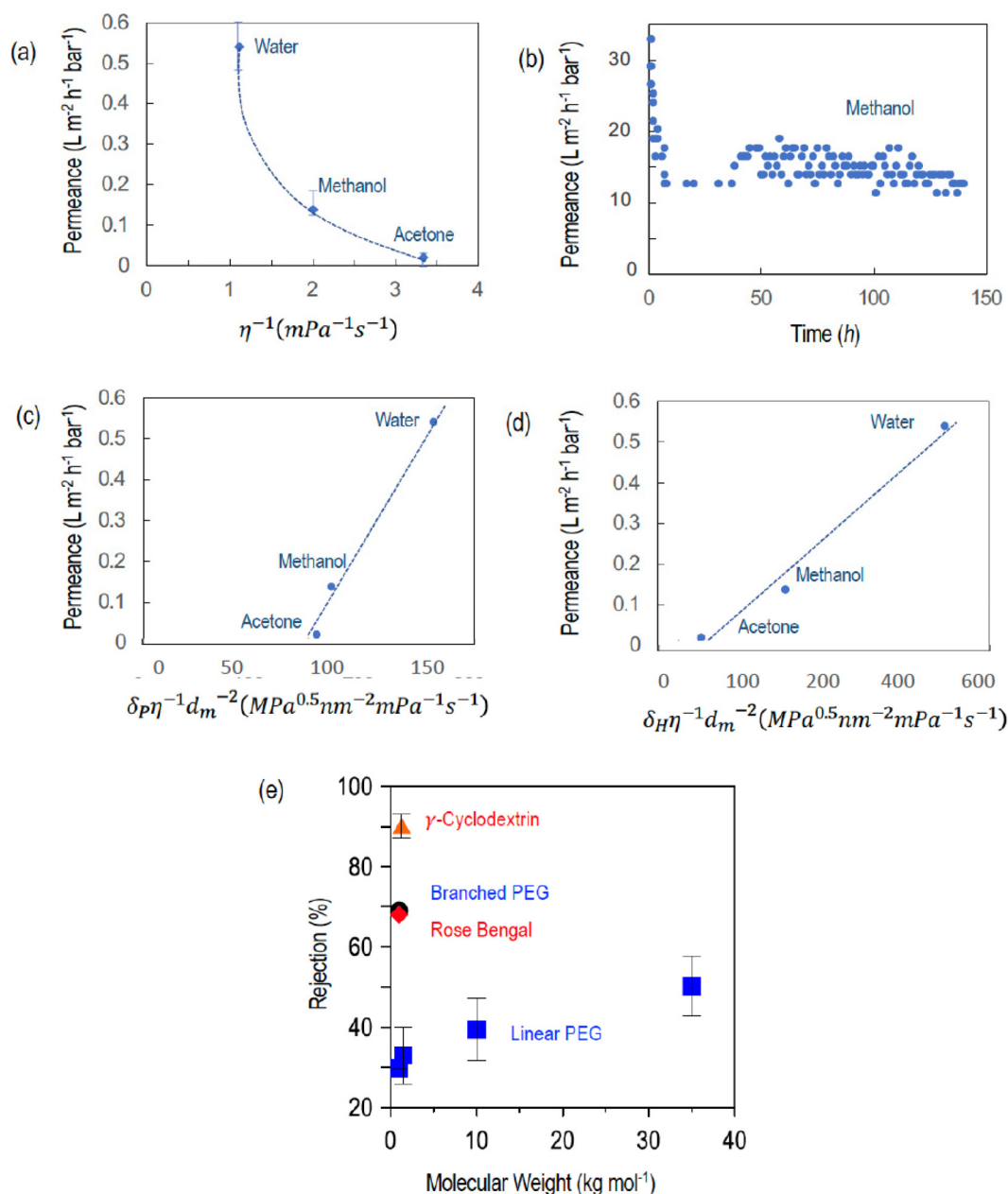


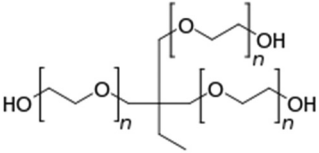
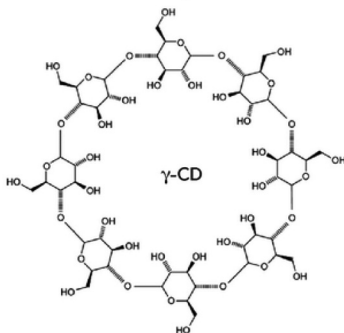
**Fig. 5** Membrane performance. (a) Solvent permeance as a function of the inverse of viscosity ( $\eta$ ). (b) Long-term methanol permeance at 19 bar. Solvent permeance as a function of the (c) polar,  $\delta_P$ , and (d) hydrogen bond,  $\delta_H$ , contributions of the Hansen solubility parameters, multiplied by the inverse of  $\eta$  and the inverse of the square of the diameter ( $d_m$ ) of the solvent molecules. (e) Rejection of different solutes dissolved in water and filtered under 19 bar at 23 °C. Membranes cast from (b) 20 wt% and (a and c–e) 22 wt% lignin in DES and subsequently crosslinked with 1,4-butanediol diglycidyl ether aqueous solution.

molecular size segregation of lignin fractions than aliphatic membranes.<sup>59</sup> Functionalized ceramic membranes (FunMem®) developed by VITO have been applied for affinity-based, molecular fractionation of lignin biorefinery. Due to the difference in affinity, an aliphatic grafted ceramic membrane allows the passage of a  $194 \text{ g mol}^{-1}$  lignin fraction (2,6-dimethoxy-4-propenylphenol) while it is retained by a membrane with a similar molecular weight cut-off but grafted with aromatic groups.<sup>59</sup> The current biodegradable membrane with

a highly aromatic structure could be applied in lignin biorefinery for molecular fractionation and organic solvent recovery.

The challenge of most commercially available organic solvent nanofiltration membranes in biorefinery is the low permeance ( $<1.3 \text{ L m}^{-2} \text{h}^{-1} \text{bar}^{-1}$ )<sup>38,39</sup> as well as their functional groups not contributing enough to the fractionation.<sup>59</sup> The membrane proposed in this work could be competitive with existing technologies as it fractionates components

**Table 4** Rejection values of solutes filtered through the membrane based on GPC analysis

Marker molecular weight (kg mol <sup>-1</sup> )	Marker molecular structure	Rejection (%)
Linear PEG		
0.4	H-(OCH <sub>2</sub> CH <sub>2</sub> ) <sub>n</sub> -OH	<8
1.0		30 ± 3
1.5		33 ± 7
10		39 ± 8
35		50 ± 7
Trimethylolpropane ethoxylate (1 kg mol <sup>-1</sup> )		69 ± 2
γ-Cyclodextrin (1.3 kg mol <sup>-1</sup> )		90 ± 2
		

**Table 5** Membrane permeance to various organic solvents and rejection of molecules larger than 800 g mol<sup>-1</sup>

Membrane	Solvent	Pressure (bar)	Permeance (L m <sup>-2</sup> h <sup>-1</sup> bar <sup>-1</sup> )	Rejection (%)	Ref.
<b>Integral asymmetric membranes</b>					
PEEKWC	Isopropanol	11	0.9	99.8% RB	42
Crosslinked PVDF	Isopropanol	—	0.34	95% RB	43
VAPEEK	Isopropanol	20	0.09	93% RB	44
VAPEEK	Acetone	10	0.3	94% SO	45
Crosslinked PTSC	Methanol	5	1.8	100% DR	46
PSU	Methanol	—	4.5	90% RB	47
PPSU	Methanol	5	0.11	63.8% RB	48
PEEKWC	Methanol	11	1.36	99.8% RB	49
SPEEK copolymer	Ethanol	4	16.3	99.9% RB	50
Crosslinked lignin	Methanol	19	0.14	90% CD	This work
<b>Thin-film composite membrane</b>					
ZIF-8/PVDF	Isopropanol	3	20	99.5% RB	51
UiO-66-NH <sub>2</sub> /Matrimid	Isopropanol	10	0.4	90% BBR	52
ZIF-8/PVDF	Ethanol	3	37.7	99.2% RB	51
Polyamide/MOF/PAN	Methanol	5	17	97.5% RB	53
Noria-TPC/PAN	Methanol	4	18	95% BBG	54
ZIF-8/PPSU	Methanol	10	3.2	88.8% RB	55
Porphyrin/PEI	Methanol	2	17	92% BBR	56

Markers: Rose Bengal (RB), 1018 g mol<sup>-1</sup>; Brilliant Blue R (BBR), 826 g mol<sup>-1</sup>; Sudan Orange (SO), 880 g mol<sup>-1</sup>; Brilliant Blue G (BBG), 854 g mol<sup>-1</sup>; Direct Red (DR), 1373 g mol<sup>-1</sup>; γ-cyclodextrin (CD), 1300 g mol<sup>-1</sup>; Direct Red (DR); Rose Bengal (RB). Membrane material: poly(ether ether ketone) (PEEK), cardo-PEEK (PEEKWC), poly(vinylidene fluoride) (PVDF), PEEK with valeric acid group (VAPEEK), metal organic framework (MOF), terephthaloyl chloride (TPC), polyacrylonitrile (PAN), polysulfone (PSU), polyphenylsulfone (PPSU), *m*-phenylene diamine (MPD), trimesoyl chloride (TMC), polyetherimide (PEI), sulfonated PEEK copolymer (SPEEK), polythiosemicarbazide (PTSC).

based on shape or size, and this kind of separation is commonly required in biorefinery. Over a prolonged run, the accumulation of viscous lignin oil combined with other pulp products is inevitable. Yet, the impact could be minimal with membranes of properties like the process fluid.

The similar property between the membrane and the process fluid could also be applied for a dedicated and controlled affinity-based fractionation of lignin derivatives, which usually have similar molecular weight and functionalities.



## Conclusion

We reported for the first time the fabrication of lignin membranes stable in organic solvents, dissolving the polymer in a green deep eutectic solvent. This is also the first time that a deep eutectic solvent is used without any co-solvent for the membrane fabrication. To increase the solvent and thermal stability of the prepared lignin membrane, a green crosslinking strategy was adopted. This methodology contributes to a more environmentally friendly route of membrane fabrication processing, using a bio-derived polymer source, greener solvents, and a non-toxic crosslinker. The crosslinking itself is performed in the aqueous medium. This work implements sustainability concepts that are in line with green chemistry principles.

The best result was obtained with membranes prepared from 22 wt% lignin dissolved in a 2 : 1 propionic acid : urea mixture cross-linked with 5% BDDE solution in water. The membrane has a molecular weight cut-off close to 1.3 kg mol<sup>-1</sup> and would be useful for the fractionation of similar size molecules in water and in organic solvents.

Membrane manufacturing processes normally use polymers and solvents from fossil sources, such as dimethylformamide or *N*-methyl pyrrolidone. We use lignin from biomass and a nontoxic DES through simple casting and green crosslinking, providing a more efficient approach towards sustainable membrane manufacturing for a variety of applications which might include separation in the pharmaceutical and petrochemical industries and biorefineries.

## Author contributions

Abaynesh Yihdego Gebreyohannes: membrane preparation, characterization, data analysis, and writing the first draft. Sandra L. Aristizábal: pristine and cross-linked lignin solid-state <sup>13</sup>C NMR, TGA and contact angle measurements, analysis, and writing. Liliana P. Silva: deep eutectic solvent preparation. Eyad Qasem: DMA measurement and analysis. Stefan Chisca: membrane crosslinking. Lakshmeesha Upadhyaya: membrane preparation. Daniyah Althobaiti: membrane preparation. João A. P. Coutinho: supervision on the deep eutectic solvent. Suzana P. Nunes: conceptualization, supervision, funding acquisition, critical reviewing, and co-writing. All authors contributed to the final version.

## Conflicts of interest

The authors declare no competing financial interest.

## Acknowledgements

This work was financially supported by King Abdullah University of Science and Technology (KAUST) (BAS/1/1057-01-01). We thank Dr Abdul-Hamid Emwas for the support in the

solid-state <sup>13</sup>C NMR analysis. L. P. Silva acknowledges FCT for her PhD grant SFRH/BD/135976/2018.

## References

- 1 D. Kim and S. P. Nunes, *Curr. Opin. Green Sustain. Chem.*, 2021, **28**, 100427.
- 2 D. Zou, S. P. Nunes, I. F. J. Vankelecom, A. Figoli and Y. M. Lee, *Green Chem.*, 2021, **23**, 9815–9843.
- 3 C. M. Rochman, M. A. Browne, B. S. Halpern, B. T. Hentschel, E. Hoh, H. K. Karapanagioti, L. M. Rios-Mendoza, H. Takada, S. Teh and R. C. Thompson, *Nature*, 2013, **494**, 169–171.
- 4 J. Brahney, M. Hallerud, E. Heim, M. Hahnenberger and S. Sukumaran, *Science*, 2020, **368**, 1257–1260.
- 5 R. Mazzei, A. Yihdego Gebreyohannes, E. Papaioannou, S. P. Nunes, I. F. J. Vankelecom and L. Giorno, *Bioresour. Technol.*, 2021, **335**, 125248.
- 6 X. Shen, P. Berton, J. L. Shamshina and R. D. Rogers, *Green Chem.*, 2016, **18**, 5607–5620.
- 7 R. Mazzei, A. Y. Gebreyohannes, E. Papaioannou, S. P. Nunes, I. F. Vankelecom and L. Giorno, *Bioresour. Technol.*, 2021, 125248.
- 8 E. Favre and A. Brunetti, in *Membrane Engineering in the Circular Economy*, ed. A. Iulianelli, A. Cassano, C. Conidi and K. Petrotos, Elsevier, 2022, pp. 35–62. DOI: [10.1016/B978-0-323-85253-1.00013-7](https://doi.org/10.1016/B978-0-323-85253-1.00013-7).
- 9 Q. Xia, C. Chen, Y. Yao, J. Li, S. He, Y. Zhou, T. Li, X. Pan, Y. Yao and L. Hu, *Nat. Sustainability*, 2021, **4**, 627–635.
- 10 Y.-T. Chen, Y.-M. Sun, C.-C. Hu, J.-Y. Lai and Y.-L. Liu, *Mater. Adv.*, 2021, **2**, 3099–3106.
- 11 S. Zhan, S. Li, X. Zhan, J. Li, J. Lei and L. Wang, *J. Appl. Polym. Sci.*, 2022, **139**, 51427.
- 12 L. G. Paterno and L. H. C. Mattoso, *J. Appl. Polym. Sci.*, 2002, **83**, 1309–1316.
- 13 A. P. Abbott, G. Capper, D. L. Davies, R. K. Rasheed and V. Tambyrajah, *Chem. Commun.*, 2003, 70–71.
- 14 A. P. Abbott, D. Boothby, G. Capper, D. L. Davies and R. K. Rasheed, *J. Am. Chem. Soc.*, 2004, **126**, 9142–9147.
- 15 R. Castro-Muñoz, F. Galiano, A. Figoli and G. Boczkaj, *J. Environ. Chem. Eng.*, 2021, 106414, DOI: [10.1016/j.jece.2021.106414](https://doi.org/10.1016/j.jece.2021.106414).
- 16 M. Taghizadeh, A. Taghizadeh, V. Vatanpour, M. R. Ganjali and M. R. Saeb, *Sep. Purif. Technol.*, 2021, **258**, 118015.
- 17 B. Jiang, N. Zhang, L. Zhang, Y. Sun, Z. Huang, B. Wang, H. Dou and H. Guan, *J. Membr. Sci.*, 2018, **564**, 247–258.
- 18 B. Jiang, N. Zhang, B. Wang, N. Yang, Z. Huang, H. Yang and Z. Shu, *Sep. Purif. Technol.*, 2018, **194**, 239–248.
- 19 S. A. Dsouza, M. M. Pereira, V. Poliseti, D. Mondal and S. K. Nataraj, *Green Chem.*, 2020, **22**, 2381–2387.
- 20 V. Vatanpour, A. Dehqan and A. R. Harifi-Mood, *J. Membr. Sci.*, 2020, **614**, 118528.
- 21 J. K. Ali, C. M. Chabib, M. Abi Jaoude, E. Alhseinat, S. Teotia, S. Patole, D. H. Anjum and I. Qattan, *Chem. Eng. J.*, 2021, **408**, 128017.



- 22 X. Tan, W. Zhao and T. Mu, *Green Chem.*, 2018, **20**, 3625–3633.
- 23 S. S. Shahabi, N. Azizi and V. Vatanpour, *J. Membr. Sci.*, 2020, **610**, 118267.
- 24 N. Mehrabi, H. Lin and N. Aich, *Chem. Eng. J.*, 2021, **412**, 128577.
- 25 F. Russo, M. Tiecco, F. Galiano, R. Mancuso, B. Gabriele and A. Figoli, *J. Membr. Sci.*, 2022, **649**, 120387.
- 26 B. Soares, A. M. da Costa Lopes, A. J. D. Silvestre, P. C. Rodrigues Pinto, C. S. R. Freire and J. A. P. Coutinho, *Ind. Crops Prod.*, 2021, **160**, 113128.
- 27 B. Soares, D. J. Tavares, J. L. Amaral, A. J. Silvestre, C. S. Freire and J. A. Coutinho, *ACS Sustainable Chem. Eng.*, 2017, **5**, 4056–4065.
- 28 S. Chisca, G. Falca, V. E. Musteata, C. Boi and S. P. Nunes, *J. Membr. Sci.*, 2017, **528**, 264–272.
- 29 S. Yang, X. Yang, X. Meng and L. Wang, *Green Chem.*, 2022, **24**, 4082–4094.
- 30 Q. Xia, Y. Liu, J. Meng, W. Cheng, W. Chen, S. Liu, Y. Liu, J. Li and H. Yu, *Green Chem.*, 2018, **20**, 2711–2721.
- 31 L.-Y. Liu, Q. Hua and S. Renneckar, *Green Chem.*, 2019, **21**, 3682–3692.
- 32 R. J. Li, J. Gutierrez, Y.-L. Chung, C. W. Frank, S. L. Billington and E. S. Sattely, *Green Chem.*, 2018, **20**, 1459–1466.
- 33 X. Zhen, H. Li, Z. Xu, Q. Wang, S. Zhu, Z. Wang and Z. Yuan, *Int. J. Biol. Macromol.*, 2021, **182**, 276–285.
- 34 L. D. Antonino, J. R. Gouveia, R. R. de Sousa Júnior, G. E. S. Garcia, L. C. Gobbo, L. B. Tavares and D. J. dos Santos, *Molecules*, 2021, **26**, 2131.
- 35 M. E. Moustaqim, A. E. Kaihal, M. E. Marouani, S. Men-La-Yakhaf, M. Taibi, S. Sebbahi, S. E. Hajjaji and F. Kifani-Sahban, *Sustainable Chem. Pharm.*, 2018, **9**, 63–68.
- 36 C. A. Smolders, A. J. Reuvers, R. M. Boom and I. M. Wienk, *J. Membr. Sci.*, 1992, **73**, 259–275.
- 37 W. Zhang, G. He, P. Gao and G. Chen, *Sep. Purif. Technol.*, 2003, **30**, 27–35.
- 38 Z. Sultan, I. Graça, Y. Li, S. Lima, L. G. Peeva, D. Kim, M. A. Ebrahim, R. Rinaldi and A. G. Livingston, *ChemSusChem*, 2019, **12**, 1203–1212.
- 39 P. Moniz, C. Serralheiro, C. T. Matos, C. G. Boeriu, A. E. Frissen, L. C. Duarte, L. B. Roseiro, H. Pereira and F. Carvalheiro, *Process Biochem.*, 2018, **65**, 136–145.
- 40 R. Mazzei, A. Yihdego Gebreyohannes, E. Papaioannou, S. P. Nunes, I. F. J. Vankelecom and L. Giorno, *Bioresour. Technol.*, 2021, **335**, 125248.
- 41 S. Karan, Z. Jiang and A. G. Livingston, *Science*, 2015, **348**, 1347–1351.
- 42 M. G. Buonomenna, G. Golemme, J. C. Jansen and S. H. Choi, *J. Membr. Sci.*, 2011, **368**, 144–149.
- 43 M. Mertens, C. Van Goethem, M. Thijs, G. Koeckelberghs and I. F. J. Vankelecom, *J. Membr. Sci.*, 2018, **566**, 223–230.
- 44 K. Hendrix, M. Van Eynde, G. Koeckelberghs and I. F. J. Vankelecom, *J. Membr. Sci.*, 2013, **447**, 212–221.
- 45 K. Hendrix, S. Vandoorne, G. Koeckelberghs and I. F. J. Vankelecom, *Polymer*, 2014, **55**, 1307–1316.
- 46 J. Aburabie, A.-H. Emwas and K.-V. Peinemann, *Macromol. Mater. Eng.*, 2019, **304**, 1800551.
- 47 A. K. Holđa and I. F. J. Vankelecom, *J. Membr. Sci.*, 2014, **450**, 499–511.
- 48 S. Darvishmanesh, F. Tasselli, J. C. Jansen, E. Tocci, F. Bazzarelli, P. Bernardo, P. Luis, J. Degreève, E. Drioli and B. Van der Bruggen, *J. Membr. Sci.*, 2011, **384**, 89–96.
- 49 M. G. Buonomenna, G. Golemme, J. C. Jansen and S. H. Choi, *J. Membr. Sci.*, 2011, **368**, 144–149.
- 50 Y. Sun, T. Sun, J. Pang, N. Cao, C. Yue, J. Wang, X. Han and Z. Jiang, *Sep. Purif. Technol.*, 2021, **273**, 118956.
- 51 A. Karimi, A. Khataee, M. Safarpour and V. Vatanpour, *Sep. Purif. Technol.*, 2020, **237**, 116358.
- 52 Z. F. Gao, Y. Feng, D. Ma and T.-S. Chung, *J. Membr. Sci.*, 2019, **574**, 124–135.
- 53 X. Cheng, X. Jiang, Y. Zhang, C. H. Lau, Z. Xie, D. Ng, S. J. D. Smith, M. R. Hill and L. Shao, *ACS Appl. Mater. Interfaces*, 2017, **9**, 38877–38886.
- 54 Z. Zhai, C. Jiang, N. Zhao, W. Dong, P. Li, H. Sun and Q. J. Niu, *J. Membr. Sci.*, 2020, **595**, 117505.
- 55 J. Dai, S. Li, J. Liu, J. He, J. Li, L. Wang and J. Lei, *J. Membr. Sci.*, 2019, **589**, 117261.
- 56 P. H. H. Duong, D. H. Anjum, K.-V. Peinemann and S. P. Nunes, *J. Membr. Sci.*, 2018, **563**, 684–693.
- 57 M. E. Jawerth, C. J. Brett, C. Terrier, P. T. Larsson, M. Lawoko, S. V. Roth, S. Lundmark and M. Johansson, *ACS Appl. Polym. Mater.*, 2020, **2**, 668–676.
- 58 N. S. Bettahalli, R. Lefers, N. Fedoroff, T. Leiknes and S. P. Nunes, *J. Membr. Sci.*, 2016, **514**, 135–142.
- 59 M. F. S. Dubreuil, K. Servaes, D. Ormerod, D. Van Houtven, W. Porto-Carrero, P. Vandezande, G. Vanermen and A. Buekenhoudt, *Sep. Purif. Technol.*, 2017, **178**, 56–65.

